A Procedure for Automated Gas Turbine Blade Fault Identification Based on Spectral Pattern Analysis

E. Loukis
Research Assistant.

K. Mathioudakis
Lecturer.

K. Papailiou
Professor.

Laboratory of Thermal Turbomachines,
National Technical University of Athens,
Athens, Greece

A method for diagnosing the existence and the kinds of faults in blades of a gas turbine compressor is presented in the present paper. The innovative feature of this method is that it performs the diagnosis automatically, that is, it gives a direct answer to whether a fault exists and what type of fault it is, without requiring the interpretation of results by a human expert. This is achieved by derivation of the values of discriminants calculated from spectral patterns of fast response measurement data. A decision about the corresponding engine status is then derived according to the values of the discriminants. In the paper, the procedure of examining the suitability of particular parameter discriminants and the constitution of a related knowledge base is described. The derivation of decisions by a computer, and on what engine condition a particular measurement data set corresponds, are then described.

1 Introduction

Development of effective gas turbine condition monitoring and fault diagnosis methods has been the target of considerable research in recent years. Whether the methods are of the gas path analysis type or based on dynamic data, such as vibrations, the aim is to take advantage of the capabilities of modern computers in order to provide a fast and reliable answer to what the condition of the engine is when measurements are available. The introduction of expert systems, in particular, has provided the possibility of integrating the data processing and decision making techniques into computerized procedures, which can provide information of direct use even to the inexperienced user.

The existence of mechanical faults can be revealed by vibration monitoring techniques, which cover a wide range of faults, as, for example, discussed by Lifson et al. (1990). On the other hand, the possibility of detecting even minor faults of individual blades has been demonstrated by Mathioudakis et al. (1991). Derivation of the decision about the existence of a fault is based on the calculation of some characteristic quantities and the user's judgment, according to the observed features and existing experience.

The methodology proposed in the present paper gives the possibility of extracting a decision about the existence of a fault by a digital computer, eliminating the need for interpretation of the results by specialized personnel. The extraction of such a decision is possible by application of pattern recognition methods. Such methods have been applied in various other domains, e.g., monitoring of bearing elements (e.g., Li and Wu, 1989), machine tools (Emel and Kannatey-Asihm, 1989), gearboxes (Barschdorff et al., 1987). Applications to turbomachinery faults related to dynamic data have first been proposed by Barschdorff (1986). The work presented there was based on features of time traces from casing accelerometers.

The work we present here is based on spectral features of measurements of various dynamic quantities, such as internal pressure, casing acceleration, and acoustic data. Its particular feature is that before applying the pattern recognition technique, the data are preprocessed in order to derive fault signatures. On the other hand, the test case analyzed consists of a commercial industrial gas turbine operating at different loads, representing thus a realistic industrial test case of application.

The way the method is organized allows its direct inclusion in an expert system. In particular, it replies to the need of obtaining computer tools for the diagnosis of specific engine problems, as identified by Doel (1990).

2 Experimental Data

The present investigation was based upon measurements on an industrial gas turbine into which different faults were introduced. The test engine was the Ruston Tornado, described by Carchedi and Wood (1982). The instrumentation layout and measurement conditions are described by Loukis et al. (1991). For completeness, we repeat here the instruments used and the examined faults.

During the experimental campaign four categories of measurement were performed simultaneously:

(*a*) Unsteady internal wall pressure, instruments PT1 to PT5. PT2 faces rotor 1, PT3 rotor 2, etc.

Contributed by the International Gas Turbine Institute and presented at the 36th International Gas Turbine and Aeroengine Congress and Exposition, Orlando, Florida, June 3–6, 1991. Manuscript received at ASME Headquarters March 4, 1991. Paper No. 91-GT-259. Associate Editor: L. A. Riekert.

(*b*) Casing vibration, with accelerometers mounted at the outside compressor casing (instruments ACC1 to ACC6).

(*c*) Shaft displacement at compressor bearings, with a Bently Nevada system.

(*d*) Sound pressure levels, with double-layer microphones.

Five experiments were performed testing the datum healthy engine and engines with the following four faults:

Fault 1. Rotor fouling: All stage 2 rotor blades were coated with textured paint in order to roughen blade surface and alter their contour, in order to simulate a fault of all the blades of a rotor.

Fault 2. Individual rotor blade fouling: Two blades of stage 1 rotor, separated by five intact blades, were coated by textured paint in order to simulate a slight individual rotor blade fault.

Fault 3. Individual rotor blade twisted: A single blade of stage 1 rotor was twisted in order to simulate a severe rotor blade fault.

Fault 4. Stator blade restaggering: two stage 1 stator blades were mistuned in order to simulate a stator fault.

All subsequent numbered references to faults in the following text will correspond to the above classification.

Tests were performed at four different engine loads: full load, half load, quarter load, and no load (termed operating point *A*, *B*, *C*, *D*, respectively, hereafter), with the intact engine as well as the faulty engines. This means that for each fault we obtain four data sets, one at each load.

3 Spectral Difference Pattern Analysis

In order to develop an automated fault identification method, it is necessary to derive some quantitative characteristics of measured signals, reflecting the presence of faults. The derivation of fault signatures in the form of spectral comparison indices has been demonstrated by Mathioudakis et al. (1991), for the case of unsteady pressure transducer measurements. This technique is used as a departing point for the methodology presented in this paper. Using this procedure, we examine not only fast response pressure measurements, but all the different dynamic measurements mentioned in the previous section.

A difference pattern (used as fault index) derived from the measured signal of an instrument is defined by the following expression:

$$p(f) = 20[\log_{10}(sp(f)) - \log_{10}(sph(f))] \qquad (1)$$

$p(f)$ is the fault index, which is thus a set of values in function of frequency, $sp(f)$ is the power spectrum of the signal of the measuring instrument from a faulty engine, $sph(f)$ is the same spectrum from a healthy engine. It is useful to remember that expression (1) was selected among several algebraic combinations of spectra of pressure measurements, by Mathioudakis et al. (1991), on the basis of two observations: This index showed high sensitivity to each examined fault and produced distinguishable forms for each fault.

The purpose of the fault index analysis we present now is: (*i*) to improve diagnostic capabilities by selecting only the most useful information contained in indices, (*ii*) to derive some scalar functions characteristic of the fault index, and (*iii*) to exploit these scalar functions for the development of a system for the classification of the fault.

3.1 Derivation of Reduced Fault Index Patterns. Inspection of the fault indices calculated for the different measuring instruments has shown that the presence of one of the examined faults results in the appearance of differentiations mainly at multiples of the shaft rotational frequency. For the case of pressure transducers, it was even found that patterns are formed that are distinguishable by visual inspection. It was therefore decided to filter out values of the indices at frequencies other than the shaft harmonics, since the most useful diagnostic information is contained at these harmonics.

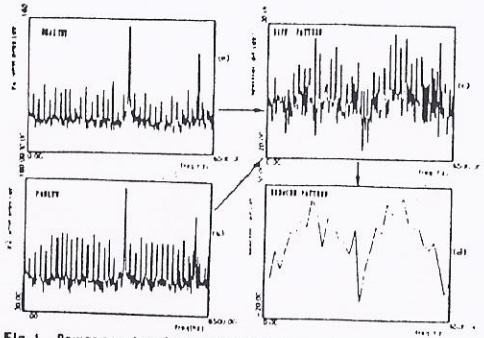

Fig. 1 Power spectra of unsteady pressure transducer 2 (PT2) with the corresponding fault index and the reduced pattern

This is done by a filter of unit gain at the rotational harmonics and zero at the other frequencies, defined by the following equation:

$$h(f) = \begin{cases} 1 \text{ if } f \text{ rotational harmonic} \\ 0 \text{ if } f \text{ not rotational harmonic} \end{cases} \qquad (2)$$

The pattern that results from filtering the difference pattern with the above filter will be referred to as *reduced pattern* in the following, and mathematically is given by the following equation:

$$p_r(f) = p(f) \cdot h(f) \qquad (3)$$

where

$p_r(f)$ = reduced different pattern at frequency f
$p(f)$ = difference pattern at frequency f
$h(f)$ = filter gain at frequency f

An example of the above procedure is given in Fig. 1. In Fig. 1(*a*) we can see the power spectrum of unsteady pressure transducer 2 in the frequency band 0-6500 Hz, for the healthy case, while Fig. 1(*b*) shows the corresponding power spectrum for Fault 4. The difference pattern and the reduced pattern are shown in Figs. 1(*c*) and 1(*d*), respectively.

It is now evident that a reduced pattern consists of a set of values $p_r(f)$, corresponding to frequencies f that are multiples of the shaft rotational frequency f_r. In the following discussion, we will refer to $p_r(f)$ as $p_r(i)$, where $p_r(i)$ is the reduced pattern at frequency if_r. If we consider an N-dimensional space with coordinates the N shaft harmonics in the considered frequency band, a reduced pattern corresponds to one point in this space (the point is defined by the values of the coordinates, which are the N values contained in $p_r(i)$).

Before introducing the discriminants derived from the reduced index patterns, we should mention the necessary features of reduced patterns that make them suitable for fault classification.

A first indication of the differentiation of the readings of a specific instrument by a fault is the amplitude of the corresponding reduced pattern (by "amplitude" we mean the range between the minimum and maximum values of the pattern). If the reduced pattern of a fault is of higher amplitude than that of another fault, this means that the transducer is more sensitive to the first fault than to the second.

On the other hand, in order to be suitable as fault signatures, the reduced patterns have to exhibit two basic features:

(*a*) Reduced patterns corresponding to one fault should be similar, when different experiments with this fault are considered.

(*b*) Reduced patterns of two different faults should be dissimilar in order to be distinguishable.

For the practical purpose of classifying patterns according to their corresponding faults, it is required that a higher degree of similarity exist between patterns of one fault, than exists between patterns of different faults.

In order to apply similarity criteria, which are objective (do not depend on the opinion of the experimenter) and quantitative (so that a computer can examine them), we introduce scalar similarity discriminants for the patterns, as explained in the following.

3.2 Reduced Pattern Discriminants. Two discriminant functions were selected, one of them expressing the quantitative similarity (influenced by both the shape and amplitude of compared patterns), the other expressing the shape similarity (influenced only by the shape of the compared patterns).

The first discriminant function is the usual Euclidean distance between reduced patterns, when they are viewed as points in an N dimensional space. It expresses the quantitative similarity between patterns, both in shape and in actual values, and for the reduced patterns P_1 and P_2 is defined by the following equations:

$$d_E(P_1, P_2) = \frac{1}{N}\sum_{i=1}^{N} (P_1(i) - P_2(i))^2 \qquad (5)$$

where $d_E(P_1, P_2)$ = Euclidean distance between the reduced patterns P_1 and P_2; $P_1(i)$, $P_2(i)$ = values of the reduced patterns P_1 and P_2 at the ith harmonic of shaft rotational frequency; N = number of rotational harmonics in the considered frequency band.

Small values of this quantity indicate that P_1 and P_2 are similar (identical if $dE(P_1, P_2) = 0$). It increases for decreasing quantitative similarity between P_1, P_2.

The second discriminant function is the normalized cross-correlation coefficient. It expresses the shape similarity between patterns and does not depend on the range of values of the patterns. For the reduced patterns P_1 and P_2, it is defined by the following equations:

$$dc(P_1, P_2) = \left| \frac{CC(P_1, P_2)}{AC(P_1) \cdot AC(P_2)} \right| \qquad (5)$$

where

$$CC(P_1, P_2) = \frac{1}{N}\sum_{i=1}^{N} (P_1(i) - \underline{P_1})(P_2(i) - \underline{P_2})$$

and

$$AC(P_k) = \left[\frac{1}{N}\sum_{i=1}^{N} (P_k(i) - \underline{P_k})^2 \right]^{1/2}, \quad k = 1, 2$$

It takes values between 0 and 1 and increases for increasing similarity between the two patterns (for patterns of identical shape, it takes the value 1).

In order to use the two discriminants for fault classification, we must possess reference patterns for each fault. If we possess such reference patterns, then for any given signal we can produce the discriminants and depending on their values we decide which is the fault corresponding to the signal. In the following paragraph we discuss how available measurement data can be judged with respect to the possibility of defining fault reference patterns.

3.3 Criteria for Measurement Suitability. In order to examine whether particular measurement data are suitable for defining reference fault patterns that are discriminable through the above functions, we apply the following procedure:

(*i*) An averaged reduced pattern of a specific fault is calculated using all available reduced patterns of this fault, from different experiments and o[illegible] points:

Fig. 2 The concept of a "well-defined pattern," visualized in a two-dimensional space

$$RP = \frac{1}{m}\sum_{i=1}^{m} P_i(i)$$

for m available experimental patterns. This is used as a reference pattern for the fault.

(*ii*) The discriminant values for all the reduced patterns (including both those coming from the examined fault and those coming from the other faults), with respect to this reference pattern are calculated.

(*iii*) Their values are inspected in order to examine if the reduced patterns of the fault are closer to the reference one, than to the reduced patterns of the other faults. This can be mathematically expressed by the following conditions:

For the Euclidean Distance (Discriminant 1):

$$\max_{k=1}^{m} d_1(RP, P_k) < \min_{j=1} d_1(RP, P_j)$$

For the Correlation Coefficient (Discriminant 2):

$$\min_{k=1}^{m} d_c(RP, P_k) > \max_{j=1} d_c(RP, P_j)$$

where RP = the average reduced pattern; P_k = the kth pattern from data from the same fault from LE experiments; P_j = the jth pattern from data from other faults, from LA experiments.

If one of these two conditions is fulfilled, the considered fault is characterized by an averaged reduced pattern, which can be distinguished from the other fault patterns. Such an average reduced pattern can be used as a signature of the fault and will be termed a *well-defined pattern* in the following.

If the reduced patterns are viewed as points in a multidimensional space, then the concept of a well-defined average reduced pattern can be expressed as the requirement of having all data points from the specific experiment within a supersphere and all the remaining points outside it. This can be visualized for a two-dimensional space, for example, as shown in Fig. 2. The points of patterns corresponding to the examined fault belong to a circle centered at average pattern, which represents the center of gravity of the points for a well-defined pattern. All the points of the other faults lie outside this circle.

In order to illustrate the application of the above procedure, it has been applied to the data from the experiments described in section 2. Conclusions as to the magnitudes and the repeatability properties of the four fault patterns are presented and discussed for all the instruments.

4 Measured Signal Features

For each fault and measuring instrument, the averaged reduced pattern is calculated from the data sets at the four operating points described in section 2.

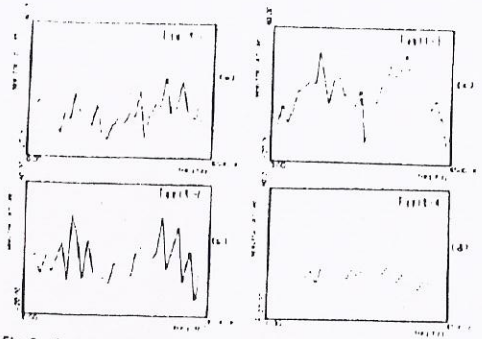

Fig. 3 Averaged patterns for each fault, derived from unsteady pressure transducer 2 (PT_2) measurements

4.1 **Unsteady Pressure Transducers.** The four average reduced patterns produced by the four faults on PT_2, facing the first stage rotor, are shown in Fig. 3. We remark that Faults 2 and 3 are characterized by high-magnitude patterns. The means that this transducer is highly sensitive to both blading faults of the rotor it faces. On the other hand Fault 1 is characterized by a lower magnitude patterns compared to Faults 2 and 3. So the transducer senses a fault of the rotor one stage downstream, but less intensively. Finally Fault 4 is characterized by a very low magnitude pattern, which means that the transducer is not sensitive to a stator fault of the same stage. This is probably due to the fact that Fault 4 is not rotating and its location although very near to the transducer axially is circumferentially 90 deg apart from it.

The values of the discriminants calculated for each reference pattern and all the available reduced patterns are shown in Fig. 4. In Fig. 4(*a*) we see the values of the Euclidean distance between the average patterns of Fault 1 on one hand and the four patterns of this fault, as well as the twelve other fault patterns, on the other. The first four patterns, corresponding to Fault 1 at operating points *A*, *B*, *C*, *D* are characterized by lower Euclidean distance values than all the other patterns. Therefore Fault 1 has a well-defined pattern on the signals of PT_2, using the Euclidean distance. We can see that the same happens with the other three faults as well.

In Fig. 4(*b*) the values of the normalized cross-correlation coefficient between the average pattern of Fault 1 on one hand and the four patterns of this fault and also the twelve other fault patterns on the other. We can remark that the first four patterns corresponding to Fault 1 at operating points *A*, *B*, *C*, *D* are characterized by higher normalized cross-correlation coefficient values than all the other patterns, corresponding to the other three faults. So Fault 1 has a well-defined pattern at PT_2 using the normalized cross-correlation coefficient. This is in agreement with what has been concluded using the Euclidean distance. In Fig. 4(*b*) we can remark that the same happens with faults 2 and 3 but not with Fault 4.

For Fault 4 using the normalized cross-correlation coefficient, the pattern of PT_2 is found to be not well defined, in disagreement with what has been found using the Euclidean distance. This can be explained taking into account that the patterns of Fault 4 are of low magnitude; therefore they are much more influenced by noise and field changes with the operating point than the other faults patterns. These factors change the shape significantly but the magnitude of the patterns does not change very much. This fact shows that examining the value of one discriminant only may not reveal all the available information.

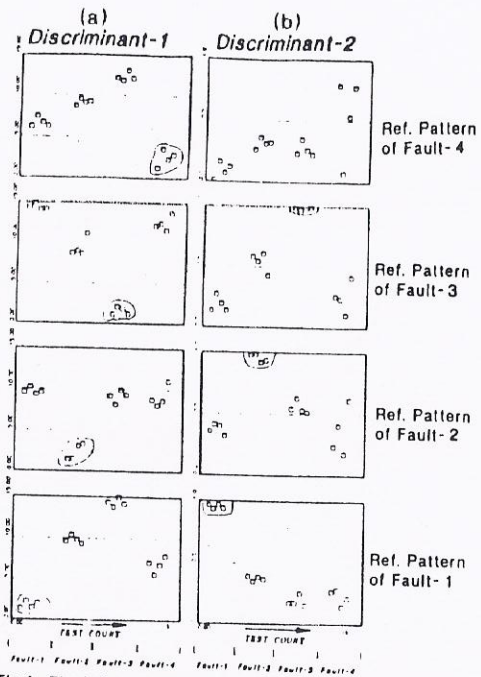

Fig. 4 Discriminant values for data from unsteady pressure transducer 2 (PT_2) measurements; all available data sets are compared to each fault reference pattern

Applying the same procedure on the data from transducer PT_5 gives the results of Fig. 5. We can remark that all faults have well-defined patterns both from the quantitative and the shape similarity point of view. However, the distances separating the clusters of points corresponding to the data of the various faults are reduced. The discriminability of faults is therefore reduced.

The procedure has been repeated for pressure transducers PT_4 and PT_6, leading to the confirmation of the conclusion that the difference patterns, although they are attenuated by traveling downstream some stages, still remain well defined.

From the above reduced pattern analysis, we come to the conclusion that a blading fault mainly influences the pressure transducer of the corresponding stage, and also influences pressure transducers several stages downstream to a lower degree.

4.2 **Accelerometers.** As a second step the accelerometers located on the external compressor casing surface were investigated. The average reduced patterns at ACC_4 are shown in Fig. 6. We remark that at ACC_4 Fault 4 is characterized by a high magnitude pattern, much higher than the same fault at PT_2. The other faults are characterized by lower magnitude patterns. Therefore this accelerometer is very sensitive to Fault 4, but shows also a lower sensitivity to the other three faults. This increased accelerometer sensitivity to Fault 4 is explained if we take into account that Fault 4 is one of stationary blading, which is mechanically connected to the compressor casing, where the accelerometers are located. Discriminant values for the data from ACC_4 are shown in Fig. 7. We remark that not only Fault 4, but the other faults as well have well-defined patterns both from quantitative and shape similarity point of

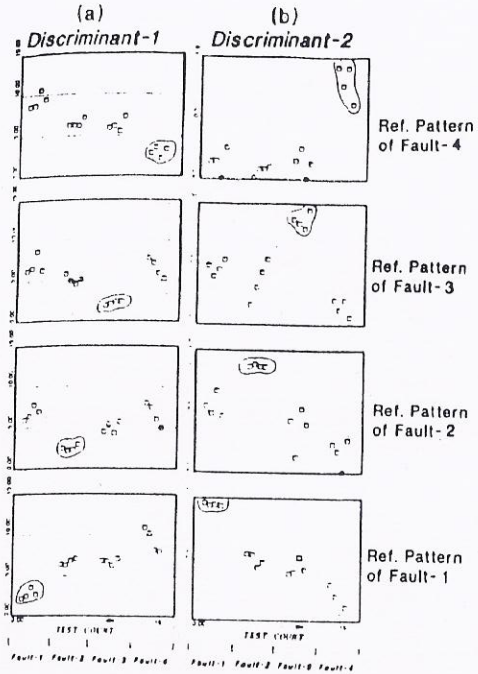

Fig. 5 Discriminant values for data from unsteady pressure transducer 5 (PT_5) measurements; all available data sets are compared to each fault reference pattern

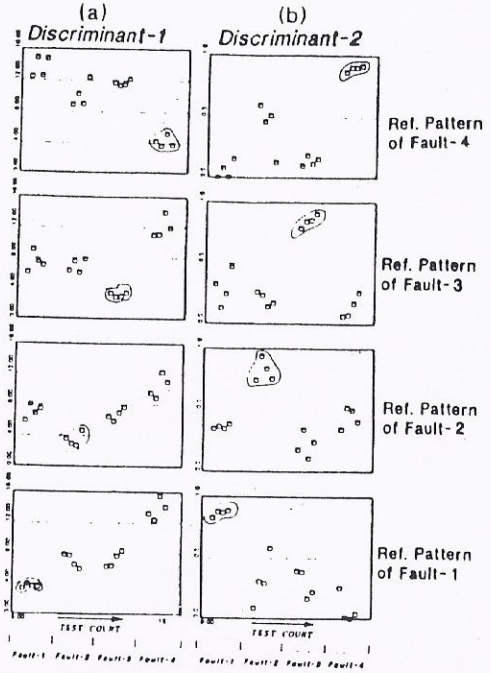

Fig. 7 Discriminant values for data from accelerometer 4 (ACC_4) measurements; all available data sets are compared to each fault reference pattern

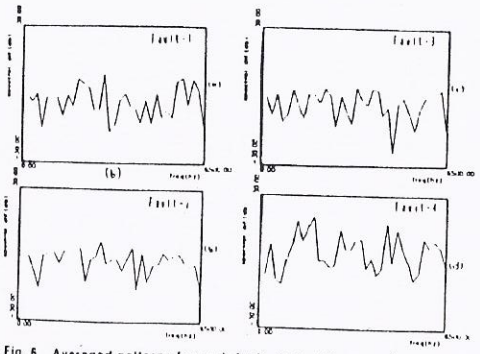

Fig. 6 Averaged patterns for each fault, derived from accelerometer 4 (ACC_4) measurements

view. Comparing to the results of Fig. 4, we can also remark that the separation of the clusters is not as clear as for PT_2.

The same procedure has been repeated for all the accelerometers. It was concluded that at all accelerometers Fault 4 has a high magnitude pattern, while Fault 3 has only at some of them high magnitude patterns, while in the others lower magnitude ones. Faults 1 and 2 have lower magnitude patterns at all the accelerometers. Also faults 3 and 4 have at all the accelerometers well-defined patterns, Fault 1 only at some of them, and Fault 2 presents well-defined patterns in none of the accelerometers.

From the above reduced pattern analysis, we conclude that the accelerometers are all influenced by Faults 3 and 4 significantly. They are also influenced by the other two faults as well, but to a lower extent, depending on the axial and the circumferential position of the accelerometer.

4.3 **Microphones.** Discriminant values for the data from one of the microphones are shown in Fig. 8. We note that Faults 2, 3, 4 have well defined patterns, but this does not happen with Fault 1. The conclusion, after repeating the same procedure for the second microphone as well, is that the microphones are influenced significantly by Faults 3 and 4, but also to a lower extent by Faults 1 and 2.

4.4 **Bearing Proximity Probes.** Discriminant values for the data from a bearing proximity probe are shown in Fig. 9. We remark that only Fault 4 has a well-defined pattern while the others do not. From examining the other bearing proximity probes as well, the conclusion that they show only some sensitivity to Fault 4, while to all the other faults they do not, is confirmed.

5 Automated Fault Diagnosis

Based on the reduced spectral patterns, and the results of the previous section, an automated fault diagnosis method has been developed. This method has as input the time trace of a specific instrument and as output the fault selection based on it. The classification algorithm used, is the minimum-distance

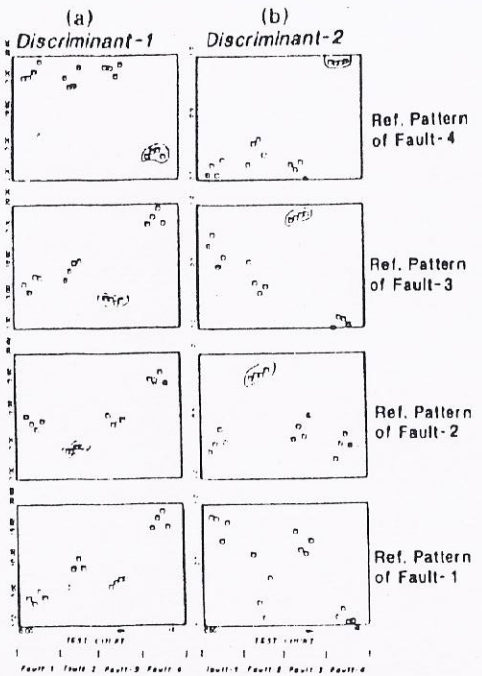

Fig. 8 Discriminant values for data from microphone measurements; all available data sets are compared to each fault reference pattern

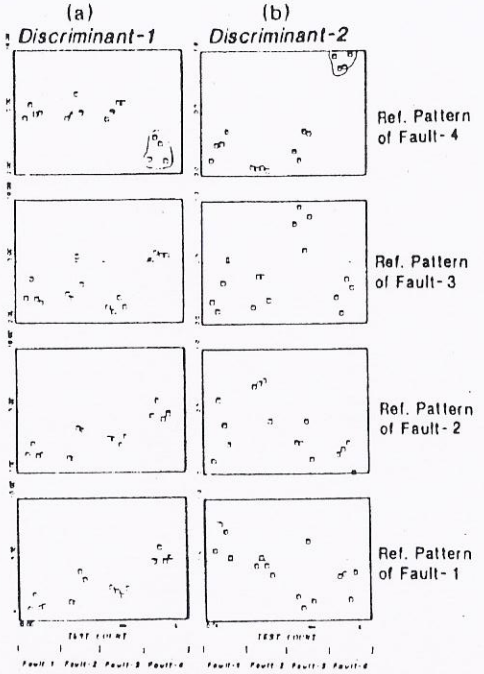

Fig. 9 Discriminant values for data from bearing proximity probe measurements; all available data sets are compared to each fault reference pattern

method (Sing-Tze, 1984), with number of classes equal to the number of faults.

For the input time trace, first the spectral density and then the reduced difference patterns are calculated. The distances of the calculated reduced pattern from the average reduced pattern of each fault are calculated, and the nearest of the faults is selected. This is given mathematically by the following expression:

For the Euclidean distance

$$I_{\text{fault}} = I \text{ for which } d_I\ (RP_I, P) \text{ is minimum}$$

For the correlation coefficient or

$$I_{\text{fault}} = I \text{ for which } d_I\ (RP_I, P) \text{ is maximum}$$

where P is the pattern under classification and RP_I reference fault patterns. The flow chart of the method is given in Fig. 10.

Typical results of its application are given for three instruments in Figs. 11–13, in order to demonstrate the principle of the method. Results for PT_3 signals are given in Fig. 11(a, b) for the Euclidean distance and the normalized cross-correlation coefficient respectively. In Fig. 11(a) we can see the results for the four patterns of Fault 1, corresponding to the operating points A, B, C, D. For each of them we can see the four Euclidean distance values from the four faults' averaged patterns. We remark that for all four patterns the first of the values, corresponding to the average pattern of the first fault, is the lowest. Therefore the above method leads to a correct selection for all four patterns using the Euclidean distance. In Fig. 11(b) we can see the same results as in 11(a), but using the normalized cross-correlation coefficient. Again we remark that for all four patterns the first of the values, corresponding

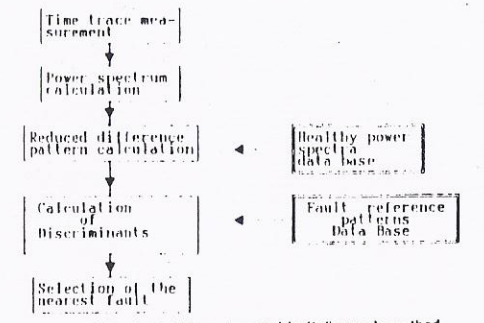

Fig. 10 Flow chart of the automated fault diagnosis method

to the average patterns of the first fault, is the highest. Therefore the above method leads to a correct selection, using the normalized cross-correlation coefficient as well.

Corresponding results for the ACC_4 are shown in Fig. 12, and for the microphone in Fig. 13. We note that for both instruments the above method leads to a correct selection, for the cases of the figures.

The above method has been applied to the experimental data, for all the instruments described in section 2. For each instrument the average reduced patterns of the four faults have been calculated and used as reference patterns. From the results for each instrument the f[illegible]uccess rates (= percentage of the reduced patterns for wi[illegible] a correct selection has been done)

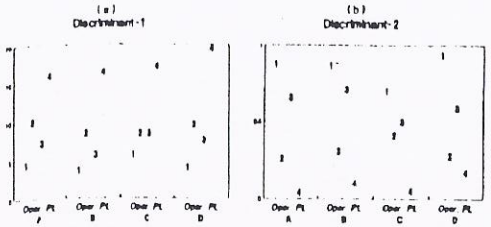

Fig. 11 Discriminant values for experimental data from PT_3, when Fault 1 is present, calculated with respect to the four reference fault patterns, for each operating point

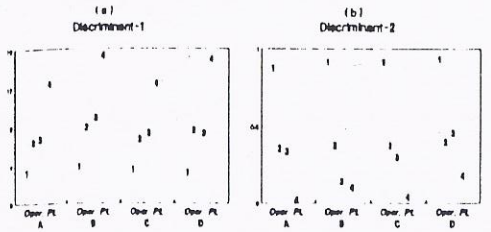

Fig. 12 Discriminant values for experimental data from ACC_4, when Fault 1 is present, calculated with respect to the four reference fault patterns, for each operating point

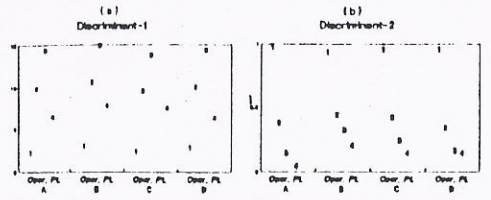

Fig. 13 Discriminant values for experimental data from microphone, when Fault 1 is present, calculated with respect to the four reference fault patterns, for each operating point

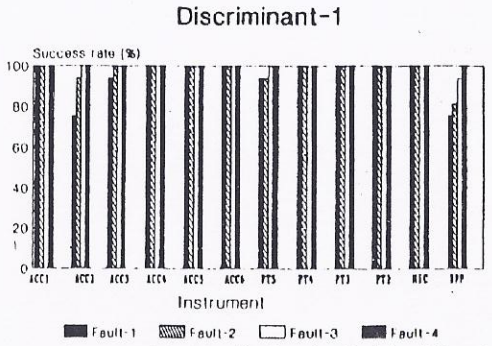

Fig. 14 Success rate in fault identification, when discriminant 1 is used

Fig. 15 Success rate in fault identification, when discriminant 2 is used

corresponding to the four faults were calculated. The table of success rates using the Euclidean distance is given in Fig. 14, and the one using the normalized cross-correlation coefficient in Fig. 15.

We can see that generally there are high success ratios for the unsteady pressure transducers, lower for the accelerometers and the microphone, while much lower for the bearing proximity probe, except for Fault 4. These differences are due to the fact that the unsteady pressure transducers are more directly influenced by the faults, while the accelerometers do not feel the fault influence directly but filtered by the compressor casing dynamics. The same happens with the microphone, which feels the fault influence filtered both by the compressor casing dynamics and the surrounding air. Finally, the bearing proximity probe feels the fault influence highly attenuated and filtered.

By comparing Figs. 14 and 15 we can see that the two discriminants do not show significant performance differences, the Euclidean distance seeming slightly better. It should be pointed out here that both these figures are based on the particular data sets we obtained. They should therefore be viewed as a measure of the effectiveness of establishing the present procedure and not as capability of the method to distinguish faults. Such a capability sh[illegible] only be tested if new data from independent experiments w[illegible] added. This statement is also valid concerning the comparative capabilities of the various instruments.

6 Discussion

The technique presented in the previous sections has been developed on the basis of the data available from experiments in an industrial gas turbine with specific implanted faults. From this point of view part of the findings can be considered of general validity while others will be particular to the specific engine.

The signatures used as a reference for the fault classification came from the experiments. While they are valid for the particular engine, it is still to be investigated whether they can be used for other engines with the same success. In that respect, it would be very useful if signatures can be produced by computer simulation, in which case a variety of engines would be covered. The research group of the authors has started work in this direction, with some success so far (see Mathioudakis et al., 1991).

On the other hand, in order to extend the present technique to other fault cases, it is necessary to obtain their corresponding signatures. Once such signatures are available, the procedure to be applied is exactly the same. This means that extension to a wider range of faults can be achieved by simply extending the data base of reference fault signatures associated with the technique.

One aspect of the present methodology that might not be of general applicability is the derivation of the reference pat-

terns. The application of the filter, which extracts information on shaft rotational harmonics, was based on our observation that blade faults produce differentiation mainly at these harmonics. This means that faults that produce differentiation only of the broad band part of the spectrum or rotor subharmonics (as for example rotating stall) would not be covered. In that case the part of the technique covering the derivation of the patterns has to be modified, by modification of the applied filter Eq. (2). In the same respect, the spectral differences of Eq. (1) can also be replaced by another expression.

A question that arises when monitoring techniques have to be applied is which are the most suitable measurements for this purpose. Although an answer to this question does not emerge from what we have presented, we have tried to include comments on the physical significance of the results obtained. Understanding this significance is helpful in choosing appropriate instruments and measuring locations. An effort to produce a systematic method of investigating this problem is under way of development.

There are certain aspects of the method that can be improved. For example, the discriminant functions were introduced here on the basis of observations and intuitions. It would be possible to establish such functions from a requirement of optimal fulfillment of certain diagnostic criteria. On the other hand, the way that decisions are taken now is of the Yes-No type. It would be desirable to include fault statistics and derive decisions of faults and associated probabilities. Work is under way in these directions by the research group of the authors.

7 Conclusions

A technique for automated fault diagnosis from dynamic measurement data has been developed.

Fault patterns were established, by manipulation of signal power spectra. Criteria for examining the suitability of the patterns for fault identification were set. A procedure for examining the possibility to establish reference patterns for each fault and each kind of measurement was presented. Having established such patterns, a technique for deciding whether a measurement signal corresponds to a particular fault was developed.

The technique was developed on the basis of experimental data coming from various instruments on an industrial gas turbine with implanted blade faults. High rates of success were found on the basis of the available data.

The present technique is such that it can be extended to include a wider range of faults, as long as additional data are available. Finally, suggestions for improving its efficiency were discussed.

References

Barschdorff, D., and Korthauer, R., 1986, "Aspects of Failure Diagnosis on Rotating Parts of Turbomachines Using Computer Simulation and Pattern Recognition Methods," presented at the International Conference on Condition Monitoring, Brighton, United Kingdom, May 21-23, Paper H1.

Barschdorff, D., 1986, "Monitoring and Expert Systems for Automatic Failure Detection," presented at the Symposium Mantenimiento Predictivo y Control de Maquinas Rotativas, Universidad de Oviedo, Gijon, Spain, July 15.

Barschdorff, D., Newman, H. E., and Nitsche, W., 1987, "Literbon Failure Diagnostics," *VDI Berichte*, No. 644, pp. 241-248.

Catchedi, F., and Wood, G. R., 1982, "Design and Development of a 12:1 Pressure Ratio Compressor for the Ruston 6 MW Gas Turbine," ASME Journal of Engineering for Power, Vol. 104, pp. 823-831.

Doel, D., 1990, "The Role of Expert Systems in Commercial Gas Turbine Engine Monitoring," ASME Paper No. 90-GT-374.

Emel, E., and Kannatey-Asibu, E., Jr., 1988, "Tool Failure Monitoring in Turning by Pattern Recognition Analysis of AE Signals," ASME *Journal of Engineering for Industry*, Vol. 110, pp. 137-145.

Li, J. C., and Wu, S. M., 1989, "On Line Detection of Localized Defects in Bearings by Pattern Recognition Analysis," ASME *Journal of Engineering for Industry*, Vol. 111, pp. 331-336.

Lifson, A., Smalley, A., Quentin, G., and Zanyk, J., 1990, "Assessing Diagnostic Techniques for Problem Identification in Advanced Industrial Gas Turbines," ASME Paper No. 90-GT-365.

Loukis, E., Wetta, P., Mathioudakis, K., Papathanasiou, A., and Papailiou, K., 1991, "Combination of Different Unsteady Quantity Measurements for Gas Turbine Blade Fault Diagnosis," ASME Paper No. 91-GT-201.

Mathioudakis, K., Papathanasiou, A., Loukis, E., Papailiou, K., 1991, "Fast Response Wall Pressure Measurement as a Means of Gas Turbine Blade Fault Identification," ASME Journal of Engineering for Gas Turbines and Power, Vol. 113, pp. 269-275.

Sing-Tze Bow, 1984, *Pattern Recognition*, Marcel Dekker Inc., New York-Basel.